

## Pattern evolution of NiSi<sub>2</sub> grown on a Si surface upon high-current pulsed Ni-ion implantation

H. N. Zhu, K. Y. Gao, and B. X. Liu\*

Laboratory of Advanced Materials, Department of Materials Science and Engineering, Tsinghua University, Beijing 100084, China

(Received 28 January 2000)

Growth of surface fractal patterns of Ni disilicide was induced by high-current pulsed Ni ion implantation into Si wafers. By increasing the substrate temperature and the supplemental Ni deposited on Si wafers, the fractal dimensions were determined and found to increase from less than 1.64, corresponding to that of cluster-diffusion-limited aggregation, to beyond the percolation threshold of 1.88, and eventually up to 2.0 of a uniform NiSi<sub>2</sub> layer on the Si surface with fine grains. The mechanism of fractal pattern evolution is discussed, based on the consideration of the dynamic process of high-current pulsed metal-ion implantation.

Metal silicides have received much attention for their potential applications in integrated circuits because of their low resistivity and high thermal stability. Of the metal silicides, NiSi<sub>2</sub> attracted both fundamental and practical interest because of its unique structural characteristics and properties, and various techniques have been developed and employed to synthesize NiSi<sub>2</sub>.<sup>1</sup> According to the published results, however, the resistivity of NiSi<sub>2</sub> formed by solid-state reaction at 750 °C is in a range of  $\sim 30\text{--}40 \mu\Omega \text{ cm}$ ,<sup>2</sup> which is about twice of that of CoSi<sub>2</sub> or TiSi<sub>2</sub>, and the high resistivity limits its practical application.

In the mid-1980s, a new ion source was invented, to the best of our knowledge, namely the metal vapor vacuum arc (MEVVA) ion source,<sup>3</sup> capable of providing almost all the metal-ion species with an average current density up to greater than  $100 \mu\text{A}/\text{cm}^2$ . Naturally, implantation of high-current metal ions into Si wafers can cause a significant temperature rise, resulting in a simultaneous thermal annealing of the Si wafers. In 1993, the MEVVA ion implantation was employed by the authors' group to successfully fabricate a number of important metal silicides, such as C54-TiSi<sub>2</sub>,<sup>4</sup> CoSi<sub>2</sub>,<sup>5</sup>  $\beta$ -FeSi<sub>2</sub>,<sup>6</sup> and ZrSi<sub>2</sub>.<sup>7</sup> Using MEVVA ion implantation the NiSi<sub>2</sub> layer with very low resistivity comparable to those of TiSi<sub>2</sub> and CoSi<sub>2</sub> was obtained, for the first time, with a specific Si substrate temperature of 380 °C, at which the size mismatch of NiSi<sub>2</sub>/Si is actually zero.<sup>8</sup>

MEVVA implantation has the following unique characteristics. Firstly, neither *in situ* heating during implantation nor postannealing was required for the formation of silicides. Secondly, the metal ions with high-current density in the MEVVA ion source are extracted in a pulse mode. The current density in a pulse is always the same, and the increase of the average (or nominal) current densities is actually done by increasing the pulse number within a unit time.<sup>9</sup> For the MEVVA source used in the present study, the pulse current density was  $7.3 \text{ mA}/\text{cm}^2$ , which is three magnitudes of order higher than that in the conventional implanter. Thirdly, the ion dose can readily be adjusted, enabling one to trace the growth kinetics of the metal silicides step by step. Taking advantage of the above characteristics, MEVVA implantation is not only a unique method for forming metal silicides or other alloy phases, but also a valuable means for studying pattern formation, because the metal atoms are

launched into the Si substrate in a very different way compared with that involved in other methods, such as various deposition techniques.<sup>10,11</sup>

To the specific Ni-Si system, the nucleation as well as growth mechanism of Ni silicide upon MEVVA ion implantation is sharply different from that involved in conventional ion beam synthesis, which has been studied thoroughly, including the reaction of the implanted Ni ions with Si, which results in separate precipitation during implantation and later a large-scale mass redistribution during Ostwald ripening upon postannealing.<sup>12</sup> It follows that the growth kinetics upon MEVVA ion synthesis is still currently an open question requiring further investigation, which is the main objective of the present study. Our study examines the evolution of the patterns consisting of the formed Ni-silicide grains from the early/intermediate stage, progressing eventually to a uniform layer on Si. We report, in this paper, the experimental observations and characterization of the formed patterns induced by high-current pulsed Ni ion implantation and a short discussion of the possible mechanism.

The silicon wafers used in this study were *p*-type Si(111) with  $8\text{--}13 \Omega \text{ cm}$ . The wafers were cut into  $1 \times 1 \text{ cm}^2$  samples and cleaned by a standard chemical procedure. A Ni overlayer of 9 or 10 nm thick was then deposited on the Si wafers for partially compensating the sputtering effect upon implantation. The wafers were then loaded on a steel-made sample holder, to which no special cooling was provided during implantation. Ni ion implantation was carried out in a MEVVA implanter with an extract voltage of 45 kV at the average current densities of 8.8, 17.6, and  $26.4 \mu\text{A}/\text{cm}^2$  to a fixed ion dose of  $2 \times 10^{17}/\text{cm}^2$ . As the implanter has no analysis magnet, the extracted Ni ions were analyzed by a time-of-flight method to consist of 30% Ni<sup>+</sup>, 64% Ni<sup>2+</sup>, and 6% Ni<sup>3+</sup>.<sup>10</sup> A thermal couple placed at the back of the wafers was used to measure the temperature rise of the substrates during implantation, and the measuring error was about  $\pm 10 \text{ }^\circ\text{C}$ . X-ray diffraction (XRD) and an energy-dispersive spectrum (EDS) were used to identify the structure and the composition of the formed silicide, respectively. A scanning electron microscope was employed to examine the surface morphology of the Si wafers after MEVVA ion implantation under various conditions. A four-point probe instrument was used to measure the electric properties of the Si samples. Besides, an

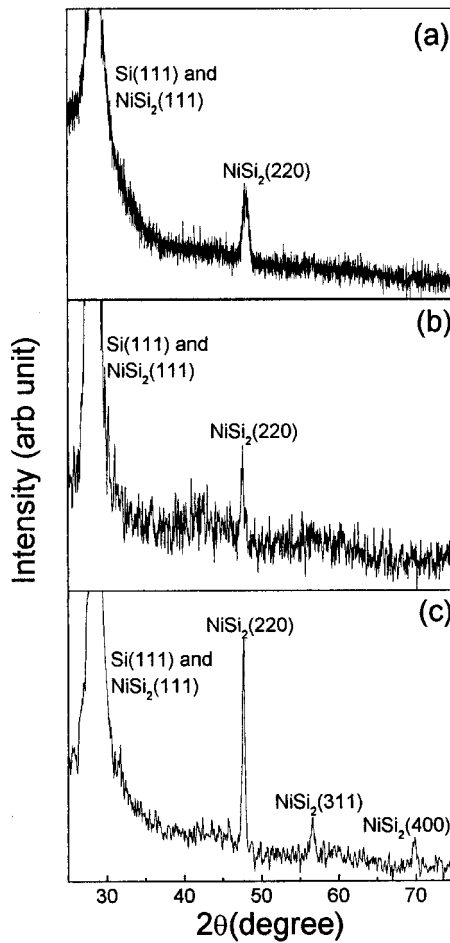


FIG. 1. The XRD patterns of the  $\text{NiSi}_2$  layers formed on the Si(111) wafers with a 10-nm Ni overlayer by MEVVA ion implantation with average current densities of (a)  $8.8 \mu\text{A}/\text{cm}^2$ , corresponding to a Si substrate temperature of  $150^\circ\text{C}$ , (b)  $17.6 \mu\text{A}/\text{cm}^2$ , corresponding to Si substrate temperature of  $240^\circ\text{C}$ , and (c)  $26.4 \mu\text{A}/\text{cm}^2$ , corresponding to a Si substrate temperature of  $310^\circ\text{C}$ .

image processing computer was used to calculate the fractal dimensions for the formed patterns on Si surface.

Figure 1 shows the XRD pattern for the Si(111) wafers covered with Ni overlayers of 10 nm thick after Ni ion implantation with three average current densities of 8.8, 17.6, and  $26.4 \mu\text{A}/\text{cm}^2$ , corresponding to the Si substrate temperatures of 150, 240, and  $310^\circ\text{C}$ , respectively. Figures 1(a) and 1(b) show that when the Si substrate temperatures were 150 and  $240^\circ\text{C}$ , respectively, only two strongest diffraction lines of (220) and (111) reflected from  $\text{NiSi}_2$  can be seen. While in Fig. 1(c), almost all the  $\text{NiSi}_2$  diffraction lines are shown, as the Si substrate temperature was raised up to  $310^\circ\text{C}$ . These

results demonstrated that  $\text{NiSi}_2$  could directly be formed by MEVVA ion implantation requiring no postannealing, and the crystallinity of the formed  $\text{NiSi}_2$  could be improved when the Si substrate temperature was raised up to  $310^\circ\text{C}$  by properly adjusting the average current density.

The sheet resistance measurements showed some unusual results. Firstly, though the XRD patterns displayed in Figs. 1(a) and 1(b) were similar, the sheet resistivity of the corresponding samples were sharply different, i.e., for the case of the Si substrate temperature being  $150^\circ\text{C}$ , the sheet resistance was too high to be measured, while for the case of  $240^\circ\text{C}$ , the sheet resistance was considerably reduced down to about  $8.1 \Omega/\square$ . Secondly, when the formation temperature was increased up to  $310^\circ\text{C}$ , the sheet resistance was  $6.0 \Omega/\square$ , which is much lower than that of the  $\text{NiSi}_2$  layers fabricated by solid-state reaction requiring a formation temperature over  $750^\circ\text{C}$ . Incidentally, the electric resistivity of the  $\text{NiSi}_2$  layers on Si wafers synthesized at a formation temperature of  $380^\circ\text{C}$  by MEVVA ion implantation could even be as low as those of  $\text{TiSi}_2$  and  $\text{CoSi}_2$ .<sup>8</sup> The x-ray diffraction analysis and sheet resistance measurement results for the Si(111) wafers covered with Ni overlayers of 9 nm thick after MEVVA ion implantation were similar to those of the Si(111) wafers with a 10 nm Ni overlayer. The characterization results for these two sets of Si wafers are summarized in Table I.

SEM examinations revealed some interesting features that emerged on the Si wafer surfaces after MEVVA ion implantation and some typical morphologies are shown in Fig. 2. One sees that at the formation temperatures of 150 and  $240^\circ\text{C}$ , surface fractal patterns emerge and they are composed of  $\text{NiSi}_2$  grains, as evidenced by above XRD and EDS analysis results. At the formation temperature of  $310^\circ\text{C}$ , the formed  $\text{NiSi}_2$  grains are a small size and cover the whole Si surface, thus forming a continuous layer. These results indicated that the average current density, i.e., the substrate temperature, affected significantly the formation of the  $\text{NiSi}_2$  phase as well as the aggregation of the  $\text{NiSi}_2$  grains on the Si surface upon high-current pulsed Ni ion implantation. To characterize the patterns, the patterns were divided into concentric disks with various radii  $R$ , and then the number of pixels  $N$  (corresponding to an area) occupied by the patterns in each disk was counted by the image processing computer. It turned out that a linear correlation could be fitted for  $\log N$  versus  $\log R$ , which corroborated that the surface patterns were indeed of fractals (see, for example, Fig. 3), and the fractal dimensions were thus obtained. For each sample, an average fractal dimension was obtained by measuring several times on a same pattern at different locations. At the formation temperature of  $150^\circ\text{C}$ , the fractal dimensions  $D$  were

TABLE I. Characterization results of Ni ion implantation into Si(111) wafers with a 9- or 10-nm-thick Ni film with varying average current density to a fixed dose of  $2 \times 10^{17}/\text{cm}^2$ . \* represents the thickness of the deposited Ni films.

Average current density ( $\mu\text{A}/\text{cm}^2$ )	Temperature rise ( $^\circ\text{C}$ )	X-ray diffraction lines of $\text{NiSi}_2$ layers	Sheet resistance ( $\Omega/\square$ )		Fractal dimension	
			9 nm*	10 nm*	9 nm*	10 nm*
8.8	150	(111)(220)	high	high	1.62	1.74
17.6	240	(111)(220)	9.2	8.0	1.88	1.94
26.4	310	(111)(220)(311)	7.0	6.0	2.0	2.0

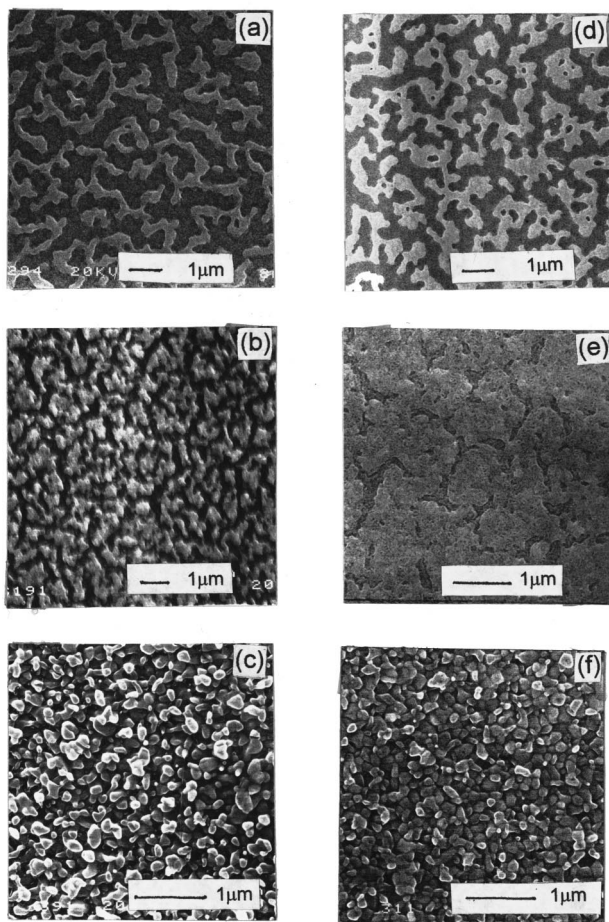


FIG. 2. The SEM morphologies of fractals of  $\text{NiSi}_2$  grown on a Si surface under high current pulsed Ni-ion implantation. (a), (b), and (c) were formed on Si(111) wafers with a 9-nm Ni overlayer; (d), (e), and (f) were formed on Si(111) wafers with a 10-nm Ni overlayer. The Si substrate temperature during implantation is (a) 150 °C, (b) 240 °C, (c) 310 °C, (d) 150 °C, (e) 240 °C, and (f) 310 °C.

1.62 and 1.74 for the Si(111) covered by a 9 and 10 nm Ni overlayers, respectively. While raising the formation temperature up to 240 °C, the fractal dimensions were increased to 1.88 and 1.94 for the Si(111) covered by 9 and 10 nm Ni overlayers, respectively, which were both around the percolation threshold. This implies that the formed  $\text{NiSi}_2$  grains become interconnected. The calculated fractal dimensions are also listed correspondingly in Table I.

As mentioned above, the MEVVA ion source provided a pulsed metal-ion beam. In the present study, the width of the pulse was 1.2 ms, and the time interval within two consecutive pulses was 0.3–1.0 s, which was much longer than the relaxation time period ( $10^{-10}$ – $10^{-9}$  s) immediately after the atomic collision triggered by implanting metal ions. The process of the MEVVA ion implantation can therefore be considered to proceed by three steps within one implanting pulse plus the time interval between the two consecutive pulses. In the first step of atomic collision, high-current Ni ion implantation launched some supplemental Ni atoms into the Si wafer, induced intermixing between the Ni overlayer and the Si

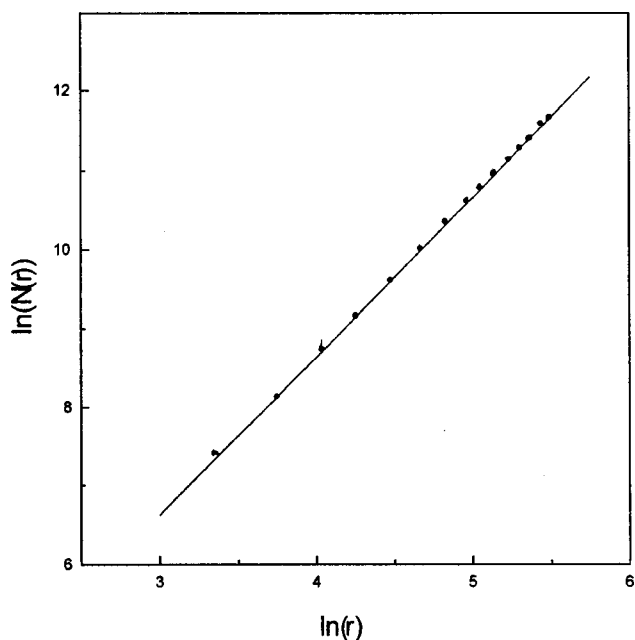


FIG. 3. Double logarithmic plot in the fractal analysis for the pattern shown in Fig. 2(a). The fractal dimension for the pattern is 1.62.

substrate, and drove the Ni-Si mixture into a highly energetic state of far-from equilibrium. It is commonly recognized that the alloy phase to be formed by implantation cannot be fixed during this step. In the second step, which began at the termination of the atomic collision, the highly energetic Ni-Si mixture should somehow relax towards equilibrium, resulting in the formation of  $\text{NiSi}_2$  grains with simplest crystalline structure as well as lowest free energy among the equilibrium Ni silicides. In the third step, the crystallized  $\text{NiSi}_2$  grains underwent a random walk and organized themselves to form some clusters. If the  $\text{NiSi}_2$  clusters could grow into a big enough size within the time interval before the next implanting pulse came, they would not be destroyed completely by the impact of the coming Ni ions. When the next pulse arrives, some new  $\text{NiSi}_2$  grains could be formed, and the growth of the previously retained  $\text{NiSi}_2$  clusters could continue to proceed. Such a course of growth can be named an intermittent (cluster diffusion-limited aggregation) process.

As the actual current density is always the same, and the interval between two consecutive pulses is much longer than the relaxation after atomic collision, the main factor that affects the formation of the silicides by MEVVA ion implantation is believed to be the substrate temperature. In addition, the sample configuration can also affect the growth of the Ni silicide as well as the pattern evolution, e.g., increasing the thickness of the predeposited Ni overlayer would increase the supplemental amount of Ni participating in the above process. Concerning the temperature effect, during the process of small-sized  $\text{NiSi}_2$  grains undergoing a random walk after they are formed, two or more small  $\text{NiSi}_2$  grains may either mix to form a cluster when they encounter each other or still keep separated. The possibility of forming a cluster is defined as the conglutination probability. It is thought that increasing the temperature will enhance the thermal motion of the  $\text{NiSi}_2$  grains and may reduce the conglutination probability among the small  $\text{NiSi}_2$  grains, i.e., may weaken the

aggregation tendency, thus resulting in a wide distribution of the aggregating NiSi<sub>2</sub> grains. It follows that upon increasing the Si substrate temperature, the fractal dimension is expected to increase, which corroborates well with the above results listed in Table I. At the highest formation temperature (310 °C) conducted in the present study, the movement of the NiSi<sub>2</sub> grains could be very violent, and the conglutination probability was decreased to zero, resulting in a uniform nucleation of NiSi<sub>2</sub> leading to a continuous layer with fine NiSi<sub>2</sub> grains on the Si surface, which corresponds to a fractal dimension of 2.0. Meanwhile, increasing the thickness of the predeposited Ni overlayer on the Si wafers resulted in the formation of more NiSi<sub>2</sub> grains, and the fractal dimension was expected to increase. This is why the fractal dimension for the case of a Si wafer covered with a 10-nm Ni overlayer was greater than for one with a Ni overlayer 9 nm thick.

In summary, we have shown that high-current pulsed Ni ion implantation into Si wafers would induce the growth of fractal patterns consisting of NiSi<sub>2</sub> grains. The fractal dimension was correlated to the substrate temperature during implantation and could also be affected a little by the thickness of the Ni overlayer. Technically, under appropriate conditions, continuous NiSi<sub>2</sub> layers on Si with fine grains can be obtained by a single-step MEVVA implantation.

The authors are grateful to the researchers at Tsinghua Electron Microscopy Laboratory and would like to thank G. W. Yang, C. Lin, and Z. C. Li for helpful discussions. This project was partially supported by the National Natural Science Foundation as well as the Ministry of Science and Technology of China. Some aid from the Institute of Semiconductors is also acknowledged.

---

\*Corresponding author. FAX: +86 10 6277 1160. Email address: dmslbx@tsinghua.edu.cn

<sup>1</sup>See, for example: S. P. Murarka, *Silicides for VLSI Application* (Academic, New York, 1983); S. Mantl, Nucl. Instrum. Methods Phys. Res. B **106**, 355 (1995).

<sup>2</sup>M. A. Nicolet and S. S. Lau, in *VLSI Electronic Microstructures Science*, edited by N. G. Einspruch (Academic, New York, 1983), Vol. 6.

<sup>3</sup>I. G. Brown, J. E. Gavin, and R. A. MacGill, Appl. Phys. Lett. **47**, 358 (1985).

<sup>4</sup>D. H. Zhu, K. Tao, F. Pan, and B. X. Liu, Appl. Phys. Lett. **62**, 2356 (1993).

<sup>5</sup>D. H. Zhu, Y. G. Chen, and B. X. Liu, Nucl. Instrum. Methods Phys. Res. B **101**, 394 (1995).

<sup>6</sup>B. X. Liu, D. H. Zhu, H. B. Lu, F. Pan, and K. Tao, J. Appl. Phys.

**75**, 3847 (1994).

<sup>7</sup>K. Y. Gao, H. N. Zhu, and B. X. Liu, Nucl. Instrum. Methods Phys. Res. B **140**, 129 (1998).

<sup>8</sup>K. Y. Gao and B. X. Liu, Appl. Phys. A: Mater. Sci. Process. **68**, 333 (1999).

<sup>9</sup>X. J. Zhang, H. X. Zhang, F. S. Sheng, S. J. Sheng, Q. Li, and Z. Z. Han, J. Beijing Normal University **28**, 148 (1992) (in Chinese).

<sup>10</sup>H. J. Gao, Z. Q. Xue, Q. D. Wu, and S. J. Pang, Solid State Commun. **97**, 579 (1996).

<sup>11</sup>M. Wang, X. Y. Liu, C. S. Strom, P. Bennema, W. Vanenckevort, and N. B. Ming, Phys. Rev. Lett. **80**, 3089 (1998).

<sup>12</sup>H. Trinkaus and S. Mantl, Nucl. Instrum. Methods Phys. Res. B **80/81**, 862 (1993).